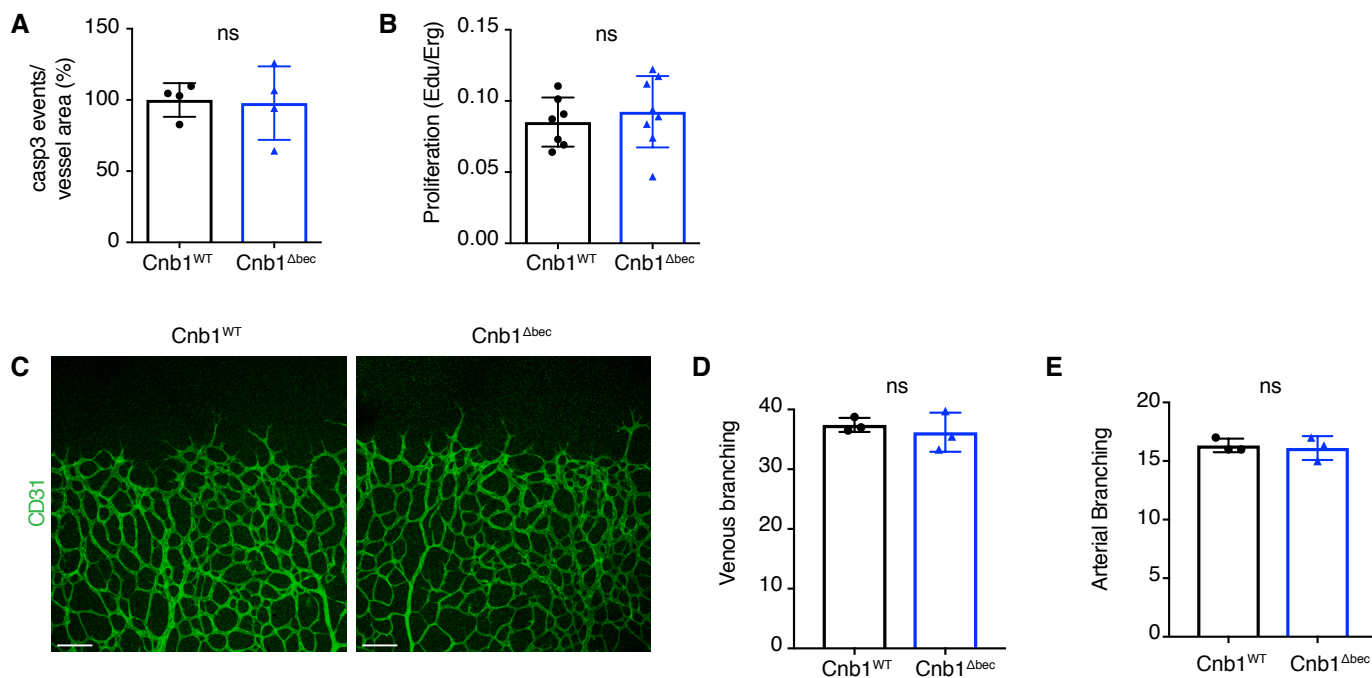**Supplemental Information**
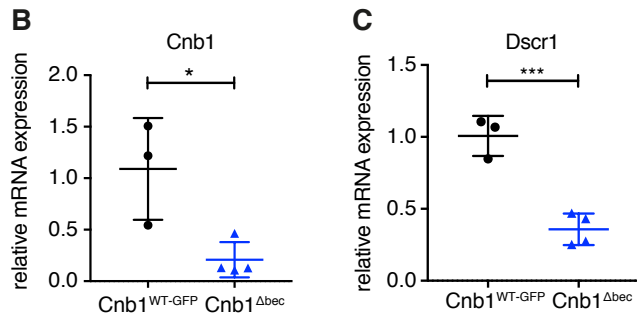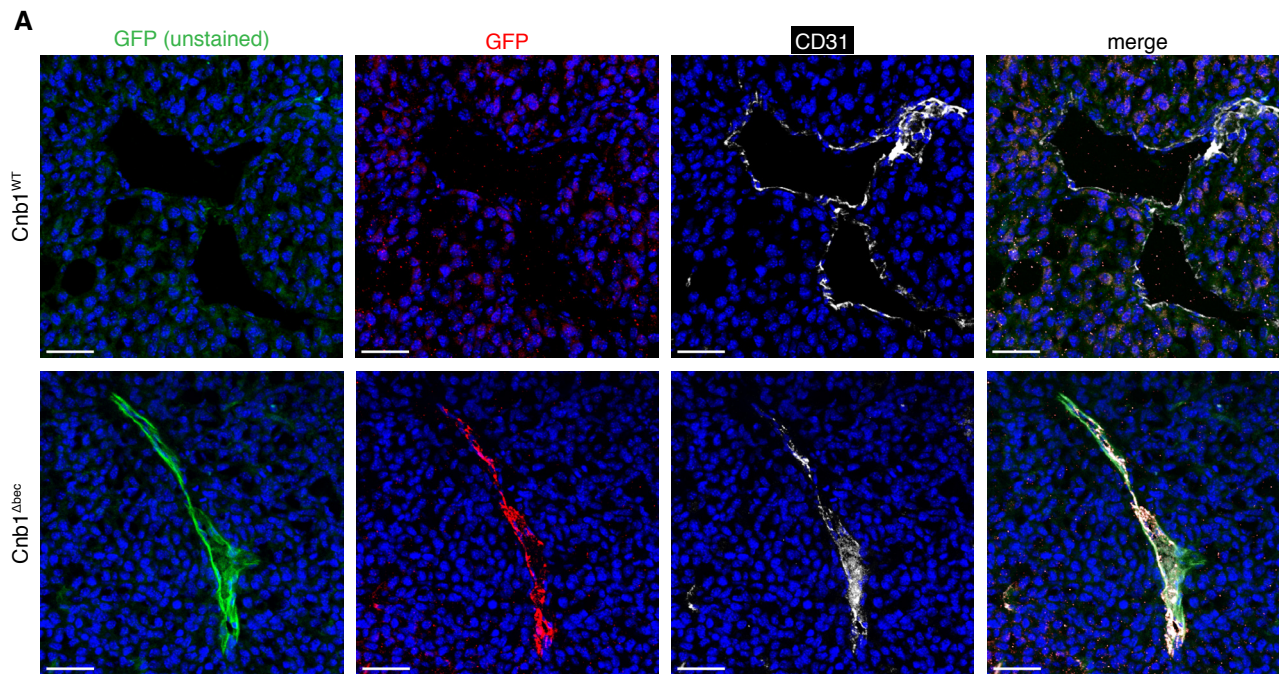
Endothelial Calcineurin Signaling Restrains

Metastatic Outgrowth by Regulating Bmp2

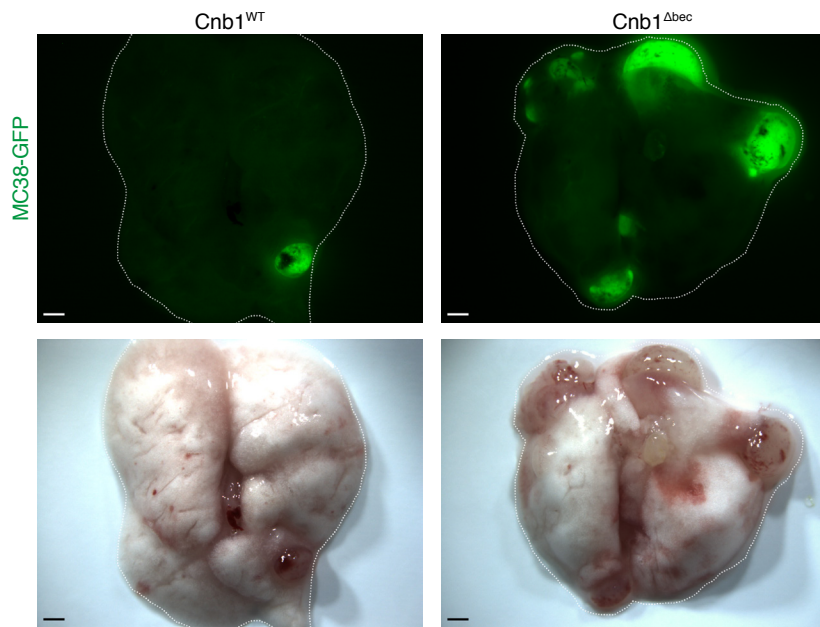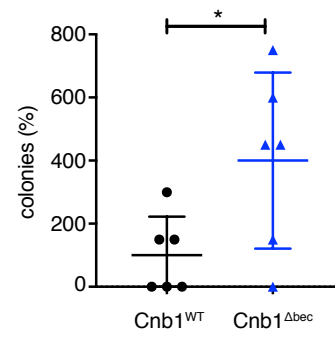Stefanie Hendrikx, Sanja Coso, Borja Prat-Luri, Laureline Wetterwald, Amélie Sabine, Claudio A. Franco, Sina Nassiri, Nadine Zangger, Holger Gerhardt, Mauro Delorenzi, and Tatiana V. Petrova
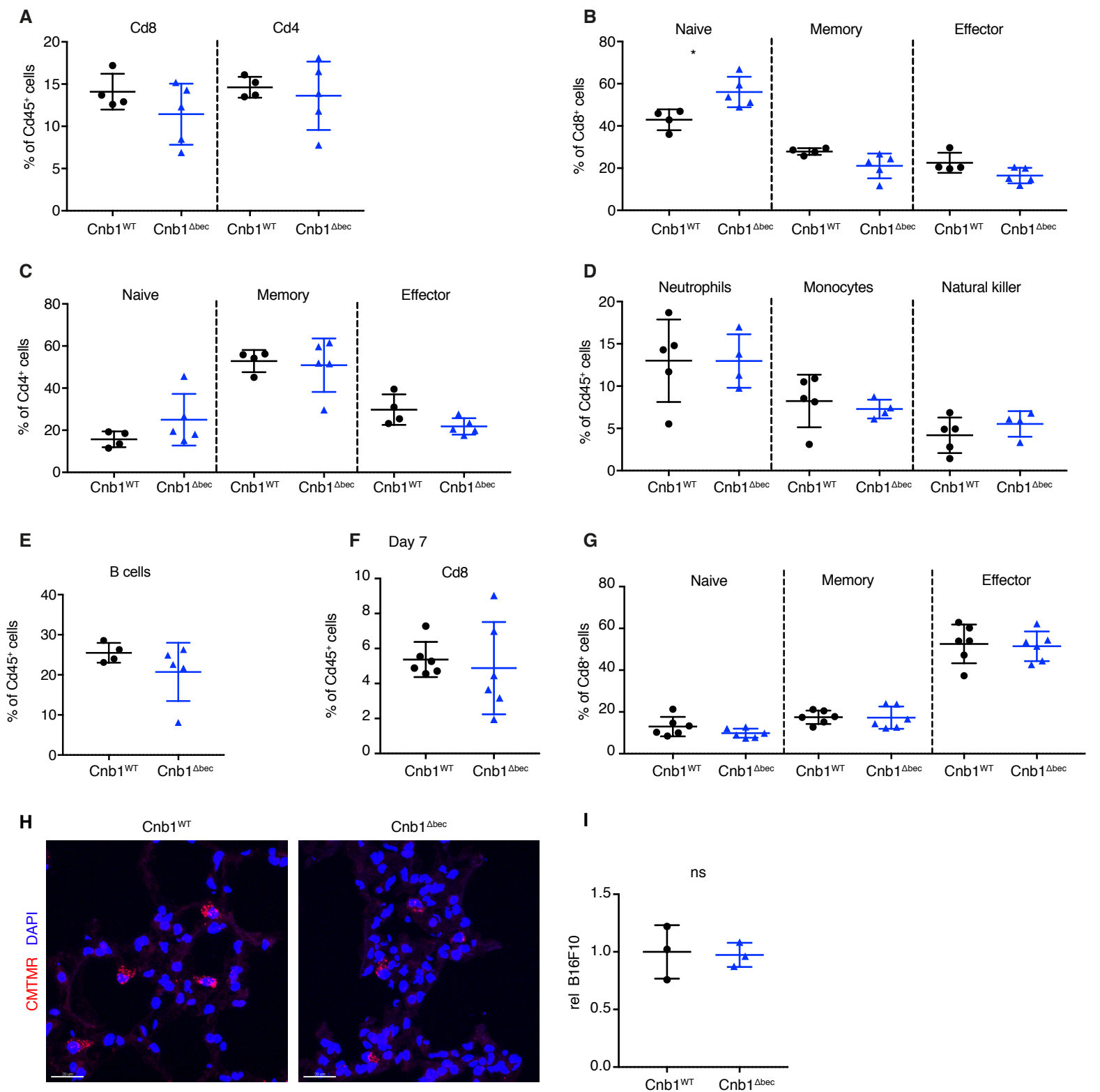
Figure S1, related to Figure 1. Endothelial calcineurin signaling does not affect sprouting angiogenesis or branching. (A) Loss of endothelial calcineurin does not affect retinal endothelial apoptosis. Quantification of caspase-3 positive cells normalized to the WT events per vascularized area (n = 4 Cnb1^{WT}; n = 4 Cnb1$^{\Delta bec}$). (B) Loss of endothelial calcineurin does not affect retinal endothelial cell proliferation. Quantification of number of proliferating endothelial cells as determined by staining for Edu and Erg (n = 7 Cnb1^{WT}; n = 8 Cnb1$^{\Delta bec}$). (C) Images of the angiogenic front of Cnb1^{WT} and Cnb1$^{\Delta bec}$ retinas. (D) Venous branching quantified as the number of vessels branching off from the vein is not affected in Cnb1$^{\Delta bec}$ retinas (n = 3 Cnb1^{WT}; n = 3 Cnb1$^{\Delta bec}$). (E) Arterial branching quantified as the number of vessels branching off from the artery is not affected in Cnb1$^{\Delta bec}$ retinas (n = 3 Cnb1^{WT}; n = 3 Cnb1$^{\Delta bec}$). ns = not significant, error bars represent mean ± SD, Two-tailed Student's t-test was performed on all data represented. Scale bar C = 100 μm.
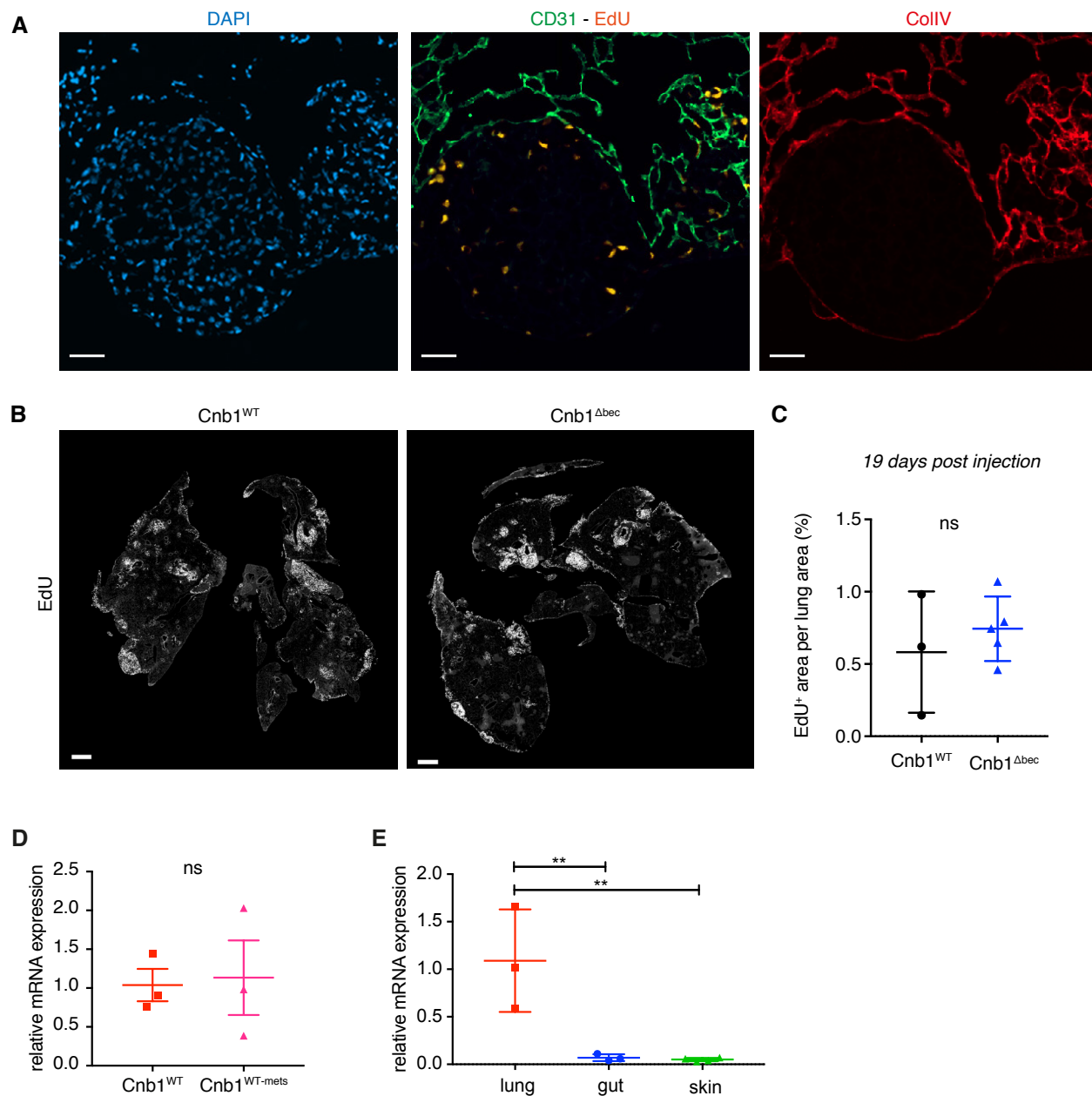
Figure S2, related to Figure 2. GFP expression and deletion efficiency of calcineurin in tumor endothelium. (A) Representative images showing EGFP and immunofluorescent staining for GFP and CD31 in Cnb1$^{\Delta bec}$ and Cnb1^{WT} tumors. As expected, GFP positive vessels in Cnb1$^{\Delta bec}$ tumors are absent in Cnb1^{WT} tumors. (B) Reduced expression of *Cnb1* in the Cnb1$^{\Delta bec}$ tumor endothelium (*p = 0.0173, n = 3 Cnb1^{WT}; n = 4 Cnb1$^{\Delta bec}$). (C) Reduced expression of *Dscr1* in the Cnb1$^{\Delta bec}$ tumor endothelium (***p = 0.0009, n = 3 Cnb1^{WT}; n = 4 Cnb1$^{\Delta bec}$). Error bars represent mean ± SD, Two-tailed Student's t-test was performed on all data represented. Scale bar: A = 100µm.

Figure S3, related to Figure 3. Endothelial calcineurin signaling restrains MC38 lung metastasis. (A) Representative images of MC38-GFP metastases in Cnb1^{WT} and Cnb1$^{\Delta bec}$ lungs. (B) Increased number of MC38-GFP colonies in Cnb1$^{\Delta bec}$ lungs, (*p = 0.0367; n = 6 Cnb1^{WT}; n = 7 Cnb1$^{\Delta bec}$). Error bars represent mean ± SD, Two-tailed Student's t-test was performed on data represented. Scale bar A = 1 mm.
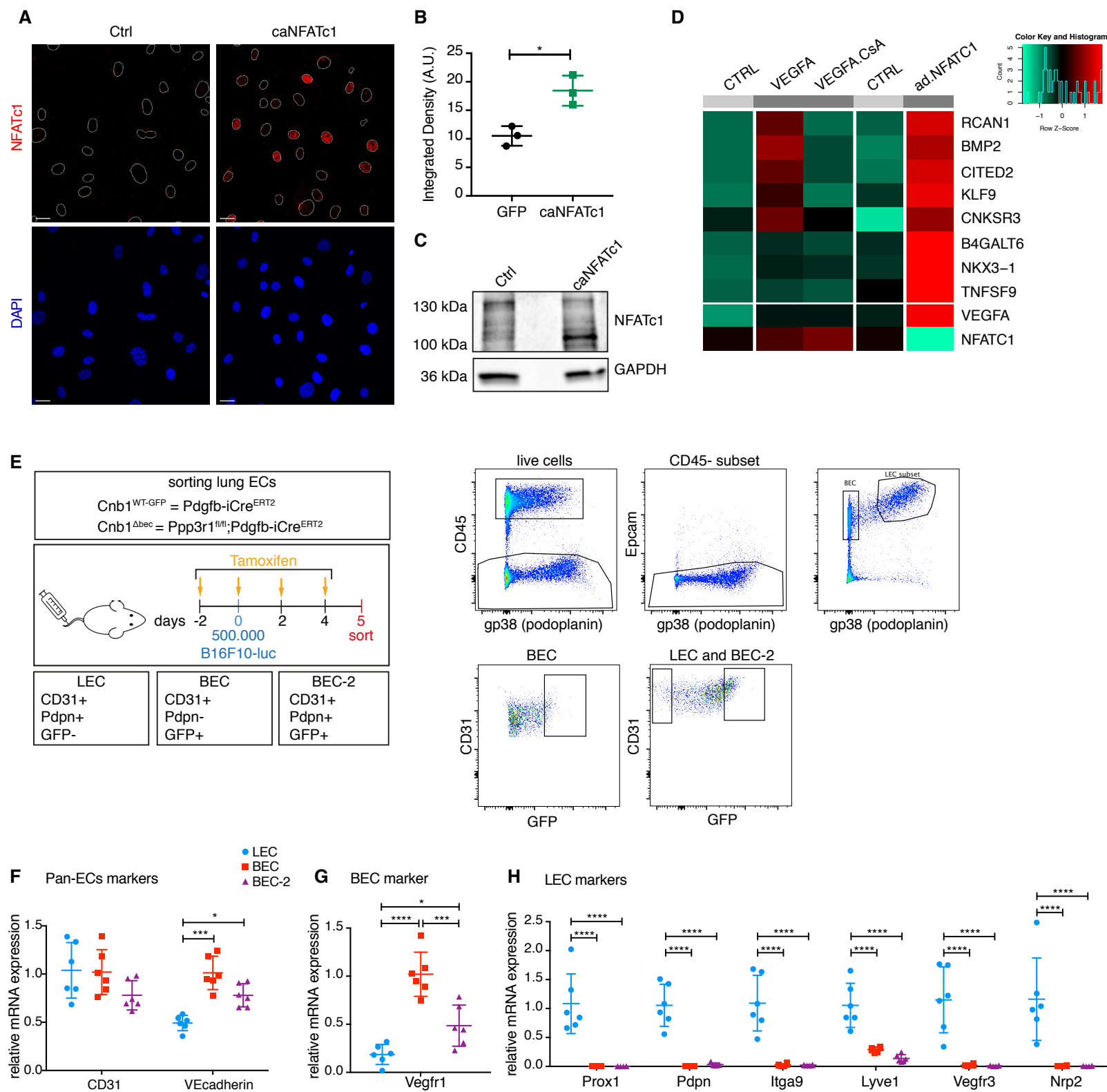
Figure S4, related to Figure 4. Immune cell populations in metastatic lungs is not affected by endothelial calcineurin deletion. (A) Comparable levels of Cd8+ and Cd4+ T cells in Cnb1^{WT} and Cnb1$^{\Delta bec}$ metastatic lungs at 5 days post i.v. injection (n = 4 Cnb1^{WT}; n = 5 Cnb1$^{\Delta bec}$). (B) Naïve Cd8 T cells were higher in Cnb1$^{\Delta bec}$ metastatic lungs, whereas no difference in central memory or effector memory Cd8 T cells was observed in Cnb1^{WT} and Cnb1$^{\Delta bec}$ metastatic lungs 5 days post i.v. injection (*p= 0.0174, n = 4 Cnb1^{WT}; n = 5 Cnb1$^{\Delta bec}$). (C) No difference in naïve, central memory or effector memory Cd4 T cells present in Cnb1^{WT} and Cnb1$^{\Delta bec}$ metastatic lungs 5 days post i.v. injection. (D) No difference was observed in neutrophils, monocytes and natural killer cells present in Cnb1^{WT} and Cnb1$^{\Delta bec}$ metastatic lungs 5 days post i.v. injection (n = 5 Cnb1^{WT}; n = 4 Cnb1$^{\Delta bec}$). (E) Comparable levels of B cells in Cnb1^{WT} and Cnb1$^{\Delta bec}$ metastatic lungs at 5 days post i.v. injection (n = 4 Cnb1^{WT}; n = 5 Cnb1$^{\Delta bec}$). (F) Comparable levels of Cd8+ T cells in Cnb1^{WT} and Cnb1$^{\Delta bec}$ metastatic lungs at 7 days post i.v. injection (n = 6 Cnb1^{WT}; n = 6 Cnb1$^{\Delta bec}$). (G) No difference in naïve, central memory or effector memory Cd8 T cells present in Cnb1^{WT} and Cnb1$^{\Delta bec}$ metastatic lungs 7 days post i.v. injection. (H) Representative images of Cnb1^{WT} and Cnb1$^{\Delta bec}$ lung sections 24h after intravenous injection of CMTMR-labeled B16F10 cells. (I) The number of B16F10 cells present in the lung 24h after i.v. injection is not affected in Cnb1$^{\Delta bec}$ mice (n = 3 per genotype). Error bars represent mean ± SD Two-tailed Student's t-test was performed for B. Scale bar H = 20μm. Error bars represent mean ± SD Two-tailed Student's t-test was performed on all data represented.
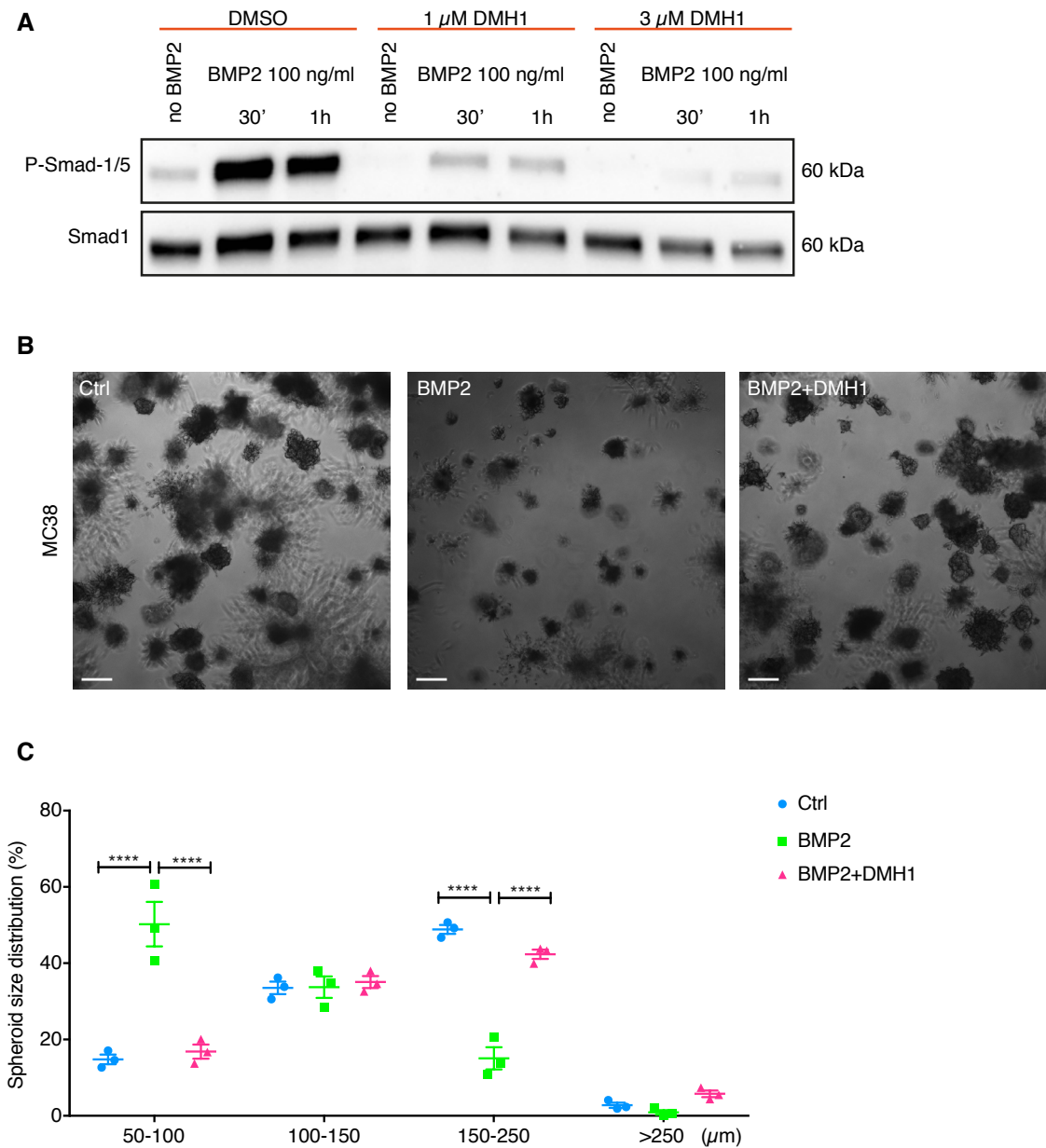
Figure S5, related to Figure 5. Vascular organization and NFAT activation in B16F10 lung metastasis. (A) Immunofluorescent staining for DAPI (blue), CD31 (green) EdU (orange) and collagen IV (red). Representative image of a B16F10 lung macrometastasis. Note mostly peritumoral CD31/collagen IV staining. EdU positive cells are mostly present at the metastatic border where B16F10 are in proximity of vessels. (B) Representative images of lung sections from Cnb1^{WT} and Cnb1$^{\Delta bec}$ mice 19 days post i.v. injection of B16F10, staining for EdU (white). (C) Macrometastases proliferation is not affected in Cnb1$^{\Delta bec}$ mice. The EdU positive area was quantified and normalized to the total lung area 19 days post i.v.injection of B16F10 cells (n = 3 Cnb1^{WT}; n = 5 Cnb1$^{\Delta bec}$). (D) *Dscr1* expression is not affected by the presence of metastasis (n = 3 Cnb1^{WT}; n = 3 Cnb1$^{WT-mets}$). (E) *Dscr1* expression is significantly higher in the lung blood endothelial cells compared to gut and skin endothelium (**$p < 0.01$, n = 3 lung; n = 3 gut; n = 4 skin). ns = non significant, error bars represent mean ± SD Two-tailed Student's t-test was performed on C and D, one-way ANOVA on E. Scale bar A = 50µm, B = 1mm.

Figure S6, related to Figure 6. Identification of calcineurin/NFAT target genes and sorting of lung ECs. (A) Representative images of HUVECs transduced with GFP or caNFATc1 lentiviruses. Staining for NFATc1 (red) and DNA (blue) after 12h of serum starvation. (B) Quantification of nuclear NFATc1 staining in HUVECs transduced with caNFATc1 or GFP (*p = 0.0121, n = 3 GFP or caNFATc1). (C) A lower motility NFAT band is present in HUVECs transduced with caNFATc1 compared to control GFP. Western blot for the indicated proteins. (D) Heat map showing differentially expressed genes induced by VEGFA without Cyclosporin A and induced by caNFATc1, but not induced by VEGFA in the presence of Cyclosporin A. Microarray data from the publically available dataset GSE49426 was used (Suehiro et al., 2014). (E) Representative FACS plots and gating scheme for sorting endothelial cells from Cnb1^WT-GFP and Cnb1^Δbec lungs, showing BECs (CD31+, GFP+, Pdpn-), LECs (CD31+, GFP-, Pdpn+) and BEC-2 (CD31+, GFP+, Pdpn+). (F) Expression of pan-endothelial population markers *CD31* and *VEcadherin* is similar in BEC, LEC and BEC-2 (*p = 0.0323, ***p = 0.0001, n = 6). (G) Expression of blood endothelial marker *Vegfr1* is increased in BEC and BEC-2 compared to LEC (*p = 0.0397, ***p = 0.0006, **** p < 0.0001 n = 6). (H) LEC markers are expressed only by LEC population (**** p < 0.0001, n = 6). Error bars represent mean ± SD Two-tailed Student's t-test was performed on data represented in B and Two-way ANOVA was performed on F-H. Scale bar A = 20μm.

Figure S7, related to Figure 6. BMP2 inhibits MC38 tumor spheroids formation. (A) BMP2 induces phosphorylation of Smad-1/5 in MC38 cells. Cells were treated with 100 ng/ml BMP2 in the presence or absence of 1 μM and 3 μM DMH1 and lysates were prepared after 30 minutes and 1h. (B) Representative images of MC38 spheroids treated with Ctrl,100 ng/ml BMP2 or 3μM DMH1. (C) BMP2 treatment increases the number of small colonies (50-100 μm) and decreased the number of bigger colonies (150-250 μm) compared to control treatment, which can be rescued by DMH1 (***$p < 0.0001$, n = 3). Error bars represent mean ± SD Two-way ANOVA was performed for C. Scale bar: B = 100 μm.